Since January 2020 Elsevier has created a COVID-19 resource centre with free information in English and Mandarin on the novel coronavirus COVID-19. The COVID-19 resource centre is hosted on Elsevier Connect, the company's public news and information website.

Virology 546 (2020) 67–78

Contents lists available at ScienceDirect

Virology

journal homepage: www.elsevier.com/locate/virology

Human mastadenovirus-B (HAdV-B)-specific E3-CR1β and E3-CR1γ glycoproteins interact with each other and localize at the plasma membrane of non-polarized airway epithelial cells

Poornima Kotha Lakshmi Narayan, Adriana E. Kajon*

Infectious Disease Program, Lovelace Respiratory Research Institute, Albuquerque, NM, USA

ARTICLE INFO

Keywords:
Human adenovirus
Mastadenovirus
Early region 3 (E3)
CR1
E3-20.1K
E3-20.5K
HAdV-B
PDZ
Class II PDZ binding Motif (PBM)

ABSTRACT

The E3 region of all simian and human types classified within species *Human mastadenovirus* B (HAdV-B) encodes two unique highly conserved ORFs of unknown function designated E3-CR1β and E3-CR1γ. We generated a HAdV-3 mutant encoding small epitope tags at the N-termini of both E3-CR1β and E3-CR1γ (HAdV-3 N-tag wt) and a double knock out (HAdV-3 N-tag DKO) mutant virus that does not express either protein. Our studies show that HAdV-3 E3-CR1β and E3-CR1γ are type I transmembrane proteins that are produced predominantly at late times post infection, are glycosylated, co-localize at the plasma membrane of non-polarized epithelial cells, and interact with each other. At their extreme C-termini HAdV-B E3-CR1β and E3-CR1γ possess a conserved di-leucine motif followed by a class II PDZ domain binding motif (PBM). HAdV-3 E3-CR1β and E3-CR1γ are dispensable for virus growth, progeny release, spread, and plaque formation in A549 cells.

1. Introduction

Human adenoviruses (HAdV) encompass more than 90 genotypes that are classified into 7 species designated *Human mastadenovirus* A through G (HAdV-A through -G) (Espinola et al., 2017; Houldcroft et al., 2018). HAdV-B comprises two subspecies, B1 and B2. In immunocompetent individuals members of subspecies HAdV-B1 and in particular types 3 and 7 are causative agents of acute respiratory disease (ARD) of variable severity (Brown et al., 1973; Chen et al., 2015; Cui et al., 2015; Hage et al., 2014; Kajon and Ison, 2016; Lin et al., 2015; Siminovich and Murtagh, 2011; Wo et al., 2015; Yamamoto et al., 2014) and also of conjunctivitis (Gopalkrishna et al., 2016; Guo et al., 1988; Martone et al., 1980). With the exception of types 14 and 55 which have been recently described as re-emerging pathogens associated with large community outbreaks of severe ARD (Cheng et al., 2018; Kajon et al., 2010, 2019; Walsh et al., 2010; Zhang et al., 2017) members of subspecies HAdV-B2 are more often detected in transplant recipients and other immunocompromised patients (Echavarria, 2008; Hofland et al., 2004; Keller et al., 1977; Stalder et al., 1977). Importantly, the genomes of several HAdV-B types including HAdV-3, -11, and -35 have been manipulated for use as oncolytic viruses and also as vectors for vaccine development and gene therapy (Chia et al., 2017; Hemminki et al., 2011; Khan et al., 2017; Li et al., 2019; Seshidhar Reddy et al., 2003; Stone et al., 2005).

The genetic determinants of the apparent higher virulence of HAdV-B have not been formally identified. The diverse genetic content of the E3 region among the genomes of human adenoviruses of species HAdV-A through HAdV-F (Burgert and Blusch, 2000; Robinson et al., 2008) has attracted considerable interest as the presence of species-specific repertoires of non-structural membrane proteins, likely evolved to subvert specific host defenses, may account for some group-specific virus host interactions underlying pathogenesis.

The species-specific E3 genes share a conserved domain (CR1) which is homologous to the RL11D domain in cytomegalovirus (Davison et al., 2003a, 2003b) and are designated CR1α, β, γ and δ based on their order in the genome. The genomes of HAdV-B, -C, -D and -E encode CR1α between E3-12.5K and E3-gp19K. Sets of 1-3 distinct species-specific HAdV E3-CR1 genes are located between the conserved E3-gp19K and E3-RIDα open reading frames (ORFs) (Fig. 1). The E3-CR1 genes are highly variable in size and sequence among species HAdV-A through –F sharing limited or no homology, and are therefore believed to encode different biological functions. The conserved E3 proteins are known to be modulators of host responses to infection. For example, E3-19K (a.k.a. gp19K) sequesters MHC class I within the endoplasmic reticulum (ER) to prevent antigen presentation and recognition of virus infected cells by cytotoxic T cells (Burgert and Kvist, 1985; Rawle et al., 1989). The receptor internalization and degradation α and β (RIDα and RIDβ) form a complex and prevent the apoptosis of

* Corresponding author. Lovelace Respiratory Research Institute, 2425 Ridgecrest Drive SE, Albuquerque, NM, 87108, USA.
E-mail address: akajon@lrri.org (A.E. Kajon).

https://doi.org/10.1016/j.virol.2020.04.005
Received 19 December 2019; Received in revised form 20 March 2020; Accepted 6 April 2020
Available online 15 April 2020
0042-6822/

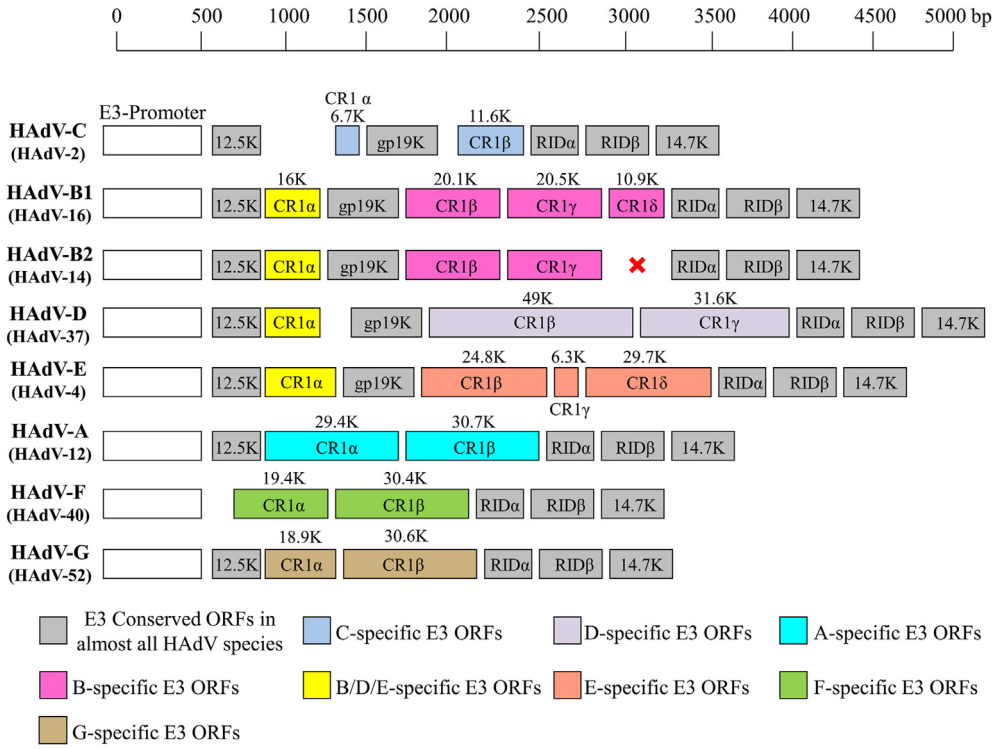

Fig. 1. Genetic content and organization of the E3 region of human adenoviruses of species HAdV-A to HAdV-G. Adapted from Burgert and Blusch, (2000) (Burgert and Blusch, 2000); **X** - ORF not present.

the infected cells by downregulating the expression of pro-apoptotic receptors FAS and TRAIL at the plasma membrane (Shisler et al., 1997; Tollefson et al., 1998, 2001). E3-14.7K blocks TNF-α-induced apoptosis of virus-infected cells (Gooding et al., 1988). In contrast, the functions of only a few E3-CR1 proteins have been identified to the present. Species HAdV-C-specific E3-CR1α (a.k.a. E3-6.7K) functions together with the RID complex to downregulate TRAIL receptors and prevent apoptosis of virus-infected cells (Benedict et al., 2001). Species HAdV-D-specific E3-CR1β (a.k.a. E3-49K) is secreted from infected cells and its N-terminus binds CD45 on leukocytes and suppresses the activation of NK cells and T cells (Windheim et al., 2013). Species HAdV-C-specific E3-CR1β (a.k.a. E3-11.6K or adenovirus death protein/ADP) facilitates virus progeny release from infected cells at late stages of infection. (Tollefson et al., 1996a, 1996b; Zou et al., 2004).

The genomes of all simian and human types classified within species HAdV-B encode two unique E3-CR1 genes designated CR1β and CR1γ which are believed to have arisen by gene duplication (Signas et al., 1986). As shown in Fig. 1, the genomes of some subspecies HAdV-B1 types encode a third highly polymorphic E3-CR1 gene designated CR1δ (Frietze et al., 2010; Kajon et al., 2005). These 3 genes have very low sequence similarity to any other known AdV genes or to other sequences in the NCBI/GenBank database, making sequence-based prediction of biological function challenging.

This paper presents the results of our initial characterization of the proteins encoded by the HAdV-B specific E3-CR1β and E3-CR1γ genes using HAdV-3 as a model.

2. Materials and methods

2.1. Amino acid sequence analysis of HAdV-B-specific E3-CR1β and E3-CR1γ

The sequences of E3-CR1β and E3-CR1γ ORFs encoded by various human and simian types classified within species HAdV-B were obtained from their corresponding whole genome sequences available from GeneBank: HAdV-3 (DQ086466), HAdV-7 (AY495969), HAdV-16 (AY601636), HAdV-21 (KF528688), HAdV-50 (AY737798), HAdV-11 (AY163756), HAdV-14 (AY803294), HAdV-34 (AY737797), HAdV-35 (AY271307), and HAdV-55 (KC857701.1), SAdV-21 (AC_000010.1), SAdV-27 (HC084988) SAdV-27.2 (FJ025928) SAdV-28.1 (FJ025914), SAdV-33 (FJ025908), and SAdV-35.2 (FJ025910.1). Multiple sequence alignments were performed using ClustalW V2.1 in Geneious v11.1.4 (Biomatters, New Zealand, https://www.geneious.com). Amino acid sequences were analyzed for the presence of functional motifs using the Eukaryotic Linear Motif resource (ELM, http://elm.eu.org/).

2.2. Cell culture

A549 cells (ATCC Cat#: CCL-185) were cultured in minimum essential medium (MEM) supplemented with 8% heat-inactivated new born calf serum (HI-NBCS, Rocky Mountain Biologicals, LLC. Missoula, MT Cat# NBS-BHT-5XM), 2.0 mM L-glutamine (Corning Inc., Corning NY Cat#: 25-005-CI), and 10 U/ml penicillin, 10 μg/ml streptomycin (Corning Inc., Corning NY Cat# 30-002-CI). Infected A549 cells were maintained in MEM supplemented with 2% HI-NBCS.

HEK 293T cells (ATCC CRL-3216) were maintained in DMEM supplemented with 10% fetal bovine serum (Rocky Mountain Biologicals, LLC, Missoula, MT Cat# FBS-BHA-5XM), 10 U/ml penicillin, and 10 μg/ml streptomycin (Corning Inc., Corning, NY Cat# 30-002-CI).

2.3. Generation of HAdV-3 mutant viruses and construction of mammalian expression vectors

For our studies, we generated a HAdV-3 mutant virus encoding small epitope tags at the N-termini of E3-20.1K and E3-20.5K (HAdV-3 N-tag wt) and a double knock-out (DKO) mutant virus that cannot express E3-20.1K and E3-20.5K (HAdV-3 N-tag DKO). For this purpose, a fragment of the E3 region mapping between nucleotides 28000 and 29800 of the genome of HAdV-3 prototype strain GB, was amplified from the genomic clone pKSB2Ad3 (Sirena et al., 2005) (a generous gift

from Dr. Silvio Hemi) and cloned into PCR blunt II-TOPO vector (ThermoFisher Scientific, Rockford, IL) to create a shuttle vector. QuikChange II XL Site-directed Mutagenesis Kit (Agilent, Santa Clara, CA Cat# 210519) was used according to the manufacturer's protocol to insert small epitope tags, VSV-G and HA into the ORFs of E3-20.1K and E3-20.5K, respectively downstream of the signal sequence (Fig. S1). The N-tag DKO mutant shuttle vector was created using the PCR blunt II-TOPO N-tag wt shuttle vector, by mutating the first and the second codons of VSV-G E3-20.1K and HA E3-20.5K to a stop codon (TGA). Subsequently, to create pKSB2HAdV-3 N-tag wt and N-tag DKO bacmids, homologous recombination was performed by electroporating pKSB2Ad3 bacmid along with the corresponding shuttle vector into BJ5183 electroporation-competent cells (Agilent, Santa Clara, CA Cat# 200154) according to the manufacturer's protocol. The recombinant bacmids were then linearized by digestion with endonuclease MluI (New England Biolabs, Ipswich, MA Cat# R0198L) and transfected individually into A549 cells using Effectene Transfection Reagent (Qiagen, Germantown, MD Cat# 301425) to generate HAdV-3 N-tag wt and HAdV-3 N-tag DKO mutant viruses. The viral genome from the newly generated mutant viruses was isolated as previously described (Kajon and Erdman, 2007) and used as a template for PCR amplification of the mutagenized portion of the E3 region using iProof High-fidelity DNA Polymerase (Bio-Rad Laboratories, Hercules, CA Cat# 172–5302). To verify the presence of tags and knock-out mutations in E3-20.1K and E3-20.5K ORFs, the amplicon was Sanger-sequenced through services contracted from GENEWIZ, South Plainfield, NJ. The sequences for the mutagenized regions of the genome of HAdV-3 in HAdV-3 N-tag wt and HAdV-3 N-tag DKO were deposited in GenBank under accession numbers MT089949 and MT089950, respectively. Schematics of the mutagenized portion of the E3 region of HAdV-3 N-tag wt and HAdV-3 N-tag DKO are shown in Fig. S2A. To further quality control the newly generated HAdV-3 N-tag wt and N-tag DKO mutants, A549 cells were infected at a multiplicity of infection (MOI) of 10 pfu/cell. At 48 h post infection (hpi), cell lysates were examined for the expression of VSV-G E3-20.1K and HA E3-20.5K by Western blot (WB) analysis (Fig. S2B).

Mammalian expression vectors pMT2-PL (Bair et al., 2017) and pMEGFP-C1 (Addgene, Watertown, MA Cat# 36412) encoding the full-length, the N-terminus, or the C-terminus of E3-20.1K or E3-20.5K with or without the transmembrane (TM) domain were generated using specific primer sets (Table S1) that amplified the corresponding domains as shown in Fig. S3. E3-20.1K and E3-20.5K class II PDZ binding motif (PBM) deletion mutants and the corresponding di-leucine motif mutants (LL/AA) in which two alanines were substituted for the two leucines (Fig. S3), were also generated using specific oligonucleotide primer sets that carried the desired mutations (Table S1).

2.4. Western blot (WB) analysis

A549 cells were infected with HAdV-3 N-tag wt or HAdV-3 N-tag DKO mutant virus at a MOI of 10 pfu/cell. At 48 hpi the cells were scraped in lysis buffer (150 mM NaCl, 50 mM Tris pH 7.4, 1% Triton X-100, and EDTA-free Protease Inhibitor Mini Tablet (ThermoFisher Scientific, Rockford, IL Cat# A32955)) and sonicated with five pulses of 22 kHz for 30 s. Protein concentration was determined with the Bio-Rad protein assay dye reagent (Bio-Rad laboratories, Hercules, CA Cat# 500-0006) according to the manufacturer's protocol. Equal amounts of protein were mixed with SDS-PAGE sample buffer, heated at 70 °C for 10 min and resolved on a 4–12% SDS polyacrylamide gel (ThermoFisher Scientific, Rockford, IL Cat# NW04120BOX). Gels were transferred to a polyvinylidene difluoride membrane (ThermoFisher Scientific, Rockford, IL Cat# 88518), blocked with 5% non-fat dry milk and probed with primary antibodies specific to the HA tag (Biolegend, San Diego, CA Cat# 9015012), VSV-G tag (Immunological Consultants Laboratories, Portland, OR Cat# RVV-45A-Z), and GAPDH (Cell Signaling Technology Danvers, MA Cat# 2118L) overnight at 4 °C. The blots were then washed 3 times with Tris-buffered saline and Tween-20 (TBS-T) and incubated with appropriate HRP-conjugated secondary antibodies (Rockland Immunochemicals Inc., Limerick PA). Protein bands were detected with SuperSignal West Femto Maximum Sensitivity Substrate (ThermoFisher Scientific, Rockford, IL Cat# 34095) and imaged using a Chemi Doc MP Imaging system (Bio-Rad Laboratories Inc., Hercules, CA).

2.5. Immunoprecipitation

pMT2-PL constructs encoding VSV-G E3-20.1K and HA E3-20.5K were transfected into HEK 293T cells either individually or together using Effectene Transfection Reagent (Qiagen, Germantown, MD Cat# 301425) according to manufacturer's protocol. At 72 h post transfection (hpt), total cell lysates were prepared as described above. Then 400 μg of protein lysate were immunoprecipitated with anti VSV-G-conjugated (Immunological Consultants Laboratories, Portland, OR. Cat# RVV-45A-Z) magnetic beads (ThermoFisher Scientific, Rockford, IL, Cat# 88802) or anti HA-conjugated magnetic beads (ThermoFisher Scientific, Rockford, IL, Cat# 88836) at 4 °C for 4 h. The immunoprecipitated samples were analyzed by WB as described above.

2.6. Glycosidase assays

The glycosylation profile of E3-20.1K and E3-20.5K was determined using a panel of N- and O-glycosidases (New England Biolabs, Ipswich, MA.). A549 cells were infected with HAdV-3 N-tag wt at a MOI 10 pfu/cell. Cell lysates were prepared as described above and 50 μg of total cell lysate were treated with PNGase F (Cat# P0708S), α2-3,6,8,9 neuraminidase A (Cat# P0722S), and O-glycosidase (Cat #P0733S) individually. Sequential treatments with α2-3,6,8,9 neuraminidase A and O-glycosidase or with PNGase F, α2-3,6,8,9 neuraminidase A, and O-glycosidase were also performed following New England Biolabs' recommended protocol. The resulting glycosylation patterns of E3-20.1K and E3-20.5K were examined using SDS-PAGE and WB analysis as described above.

2.7. Fluorescence microscopy

A549 cells were seeded on glass coverslips coated with Rat Tail Collagen 1 (Corning Inc., Corning NY Cat# 354236). The next day, cells were infected with HAdV-3 N-tag wt at a MOI of 10 pfu/cell. At different times pi cells were fixed with 4% paraformaldehyde, quenched with 0.1 M glycine, permeabilized with 0.5% Triton X-100, and blocked with 2% Bovine Serum Albumin in SuperBlock blocking buffer (ThermoFisher Scientific, Rockford, IL Cat#37515). Cells on coverslips were subsequently incubated with appropriate primary antibodies specific to VSV-G (Immunology Consultants Laboratory, Inc. Portland, OR Cat# RVV-45A-Z), HA (Biolegend, San Diego, CA Cat# 901502), Golgin-97 (ThermoFisher Scientific, Rockford, IL Cat# A-21270), EEA1 (Cell Signaling Technology, Danvers, MA Cat# 3288), prolyl 4-hydroxylase (P4HB)/protein disulfide-isomerase (PDI) (Abcam, Cambridge, MA Cat# ab2792), LAMP2 (Developmental Studies Hybridoma Bank, Iowa City, IA Cat# HB4B), or E-cadherin (R&D Systems, Minneapolis MN Cat# AF648) overnight at 4 °C. Coverslips were then washed 3 times with PBS and incubated with appropriate secondary antibodies conjugated to Alexa Fluor 488 (Jackson ImmunoResearch Laboratories, Inc. West Grove, PA, Cat# 715-546-150) or Alexa flour 647 (Jackson ImmunoResearch Laboratories, Inc. West Grove, PA, Cat# 711-606-152) for 2 h at room temperature. Coverslips were subsequently washed with PBS and mounted on microscope slides using ProLong Diamond Antifade Mountant with DAPI (Thermo Scientific, Rockford, IL Cat# P36962). Cells were imaged with a Zeiss LSM800 AiryScan confocal microscope at the University of New Mexico's Fluorescence Microscopy Resource Facility.

2.8. Gene expression analysis

A549 cells were infected with HAdV-3 N-tag wt virus at a MOI of 10 pfu/cell. At different times pi total RNA was extracted from infected cells using the RNAqueous kit (ThermoFisher Scientific, Rockford, IL, Cat# AM1912) following the manufacturer's protocol. To remove any residual contaminating DNA, 20 μg of total RNA were treated with Turbo DNA-free kit (ThermoFisher Scientific, Rockford, IL, Cat# AM1907). The complete elimination of residual DNA was verified by PCR amplification of the conserved ribosomal subunit Rig/S15 gene using primers Fw (5′ TTC CGC AAG TTC ACC TAC C 3′) and Rv (5′ CGG GCC GGC CAT GCT TTA CG 3′) and GoTaq Flexi DNA Polymerase (Promega, Madison, WI Cat# M7806) according to manufacturer's protocol. Next, Retroscript Reverse Transcription kit (ThermoFisher Scientific, Rockford, IL, Cat# AM1710) was used to reverse-transcribe 1 μg of DNAse-treated RNA. The cDNA was then used as a template for amplification with either internal primers E3-20.1K Fw 5' CCA TAT TAC CTT AGG ACA TAA TCA CAC 3'+ Rv 5' GTG CCA TTC CCA ATG 3'; and E3-20.5K Fw 5' CCT TGC AGC TGT AAC TTA TGG 3'+ Rv 5' AAT CCC ACT ACC ACG GC 3', or junction primers E3-20.1K Fw 5' CAA TCG CAA GCA TGG CTT C 3'; or E3-20.5K Fw 5' CAA TCG CAA GAT GAT TTC CAC TAC 3' + the corresponding internal Rv primers. The Forward and reverse primers of E3-20.1K and E3-20.5K internal primers anneal to specific sequences within the corresponding ORFs. The forward junction primer anneals to a specific sequence at the junction of tripartite leader sequence (TPL) and 5'end of E3-20.1K or E3-20.5K ORF. The reverse junction primer is the same as reverse internal primer. The use of junction primers allowed the specific detection of major late promoter (MLP) transcripts carrying the TPL sequence at their 5' end. The constitutively expressed Rig/S15 was amplified as a housekeeping control using the primers described above. The cycle number for amplification of all CR1 genes and Rig/S15 was optimized empirically and set at 20 to fit within the exponential range of amplification. The amplification products were analyzed by horizontal electrophoresis on 1% agarose gels. Quantitative PCR (qPCR) was performed on the same set of cDNA samples in a QuantStudio5 instrument (ThermoFisher Scientific, Rockford, IL) with PowerUp SYBR Green Master Mix (ThermoFisher Scientific, Rockford, IL Cat# A25741) and the internal and junction primer sets and the Rig/S15 primers described above. Each sample was tested in duplicate. The data were normalized to Rig/S15. Fold changes in gene expressions relative to the 0 h time point were determined using the $2^{-\Delta\Delta Ct}$ method.

2.9. Plaque assay

Confluent A549 cells seeded in a 6-well plate were infected with 100 μl of serially diluted virus sample. After adsorption for 1 h at 37 °C cell monolayers were overlaid with 1.4% low melt agarose (G-Biosciences, St. Louis, MO Cat# RC-008) mixed with an equal volume of 2X MEM supplemented with 4% HI-NBCS, 4.0 mM L-glutamine (Corning Inc., Corning NY Cat#: 25-005-CI), and 20 U/ml penicillin, 20 μg/ml streptomycin (Corning Inc., Corning NY Cat# 30-002-CI) and, 25 mM $MgCl_2$. The agarose overlay was allowed to solidify at room temperature for 20 min. A second overlay was applied 4 days pi. At 8 days pi the infected monolayers were fixed with 1% formaldehyde in 0.15 M NaCl and stained with crystal violet after removal of the agarose overlay plug. Cell monolayers were then washed and air-dried, and the plaques were counted. Infectious virus titers were determined in technical triplicates and expressed as pfu/ml.

2.10. Virus progeny release assay

Confluent A549 cells seeded in a 35 mm dish were infected with HAdV-3 wt, HAdV-3 N-tag wt, or HAdV-3 N-tag DKO at a MOI of 1 pfu/cell. At different times pi supernatants from infected cell monolayers (extracellular virus) were collected, transferred to a 15 ml conical tube and spun down at 1000 rpm for 10 min to remove floating cells and cell debris. For assessment of total infectious virus loads, cell monolayers along with the corresponding supernatants were transferred to a 15 ml conical and subjected to 3 cycles of freeze-thaw at −80 °C. The suspension was then clarified by spinning at 1000 rpm for 10 min to remove cell debris. Infectious virus titers were then determined by plaque assay on A549 cells as described above. Three independent experiments were performed and each experiment had biological triplicates.

2.11. Virus dissemination assay

Virus dissemination (a.k.a. spread) assays were performed as described (Doronin et al., 2003). Briefly, confluent A549 cells seeded in a 24-well dish were infected with HAdV-3 wt, HAdV-3 N-tag wt, or HAdV-3 N-tag DKO at MOIs of 10, 1, 0.1, 0.01, and 0.001 pfu/cell. At 7 days pi the cells were fixed with 4% formaldehyde in 0.15 M NaCl and stained with crystal violet for visualization of cytopathic effect.

2.12. Plaque size assay

A549 cells were infected with approximately 10–20 pfus of HAdV-3 wt, HAdV-3 N-tag wt, or HAdV-3 N-tag DKO virus. After 1 h adsorption at 37 °C the infected monolayers were overlaid as described above. At 8 days pi, the plaques were imaged at 4X magnification with an CKX41 Olympus microscope equipped with an Infinity 2–3 digital camera (Teledyne Lumenera, Canada) using the Infinity Capture software. ImageJ software (https://imagej.net) was used to measure the diameter of 70 plaques for each of the examined viruses.

2.13. Statistical analysis

All experiments were performed in biological triplicates. Graph Pad Prism V5 was used to conduct statistical analyses. Statistical significance was evaluated by one-way ANOVA and Bonferroni post-hoc test. A p value of < 0.05 was considered significant.

3. Results

3.1. E3-CR1β and E3-CR1γ are conserved among human and simian members of species HAdV-B

The alignment of predicted polypeptide sequences of E3-CR1β and E3-CR1γ encoded by various HAdV-B types revealed that the two proteins are highly conserved (Fig. 2). Importantly, the conservation of sequence and basic predicted features extends to adenoviruses isolated from great apes and classified as members of species HAdV-B (Fig. S4). The ELM tool predicted E3-CR1β and E3-CR1γ to be type I transmembrane proteins with a large N-terminal domain and a short C-terminal tail. At the N-terminal domain both proteins have a signal sequences and putative N-glycosylation sites. At the extreme C-terminus both proteins have a highly conserved di-leucine motif (LL) followed by a class II PSD95/DLG/ZO-1 (PDZ) binding motif (PBM) (consensus sequence XΦXΦ, where X = any amino acid, and Φ = any hydrophobic amino acid) (Fig. 2). The C-terminal domain of E3-CR1β also has a canonical tyrosine-based sorting motif (YXXΦ, where X = any amino acid, and Φ = any hydrophobic amino acid) which is conserved among all the examined HAdV-B types except SAdV-21, SAdV-35.2, and SAdV-27 (Fig. S4). The Src Homology 3 (SH3) domain binding motif (PXXP, where X is any amino acid) at the C-terminal domain of E3-CR1β is present in all of the examined HAdV-B types with the exception of HAdV-14 and HAdV-55 (Figs. 2 and S4).

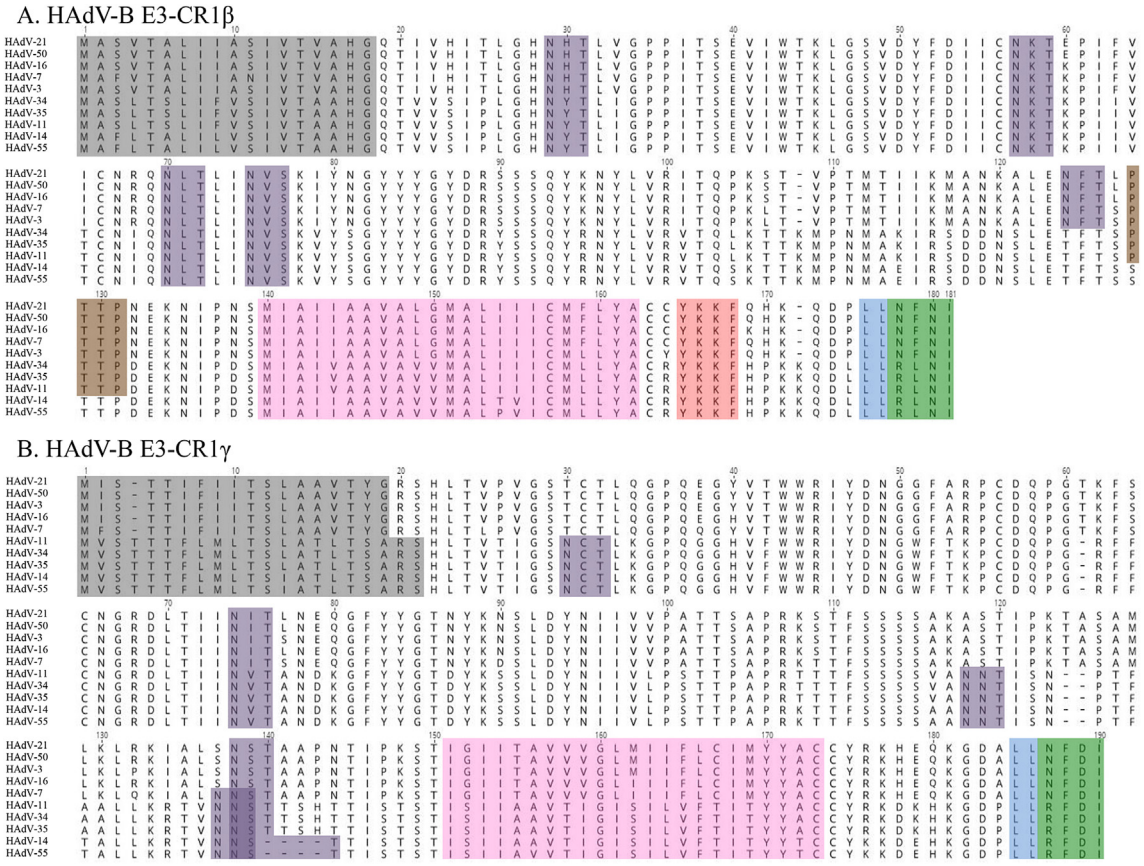

Fig. 2. Amino acid sequence analysis of HAdV-B-encoded E3-CR1β and E3-CR1γ and their predicted functional motifs: Amino acid sequences of A) E3-CR1β and B) E3-CR1γ from various HAdV-B types were aligned using ClustalW. Functional motifs were predicted using the Eukaryotic Linear Motif resource (ELM, http://elm.eu.org/). The predicted signal sequence is highlighted in grey. The N-terminal lumenal domain is separated from the short C-terminal cytoplasmic tail by a transmembrane domain (TM) highlighted in pink. Predicted glycosylation sites are highlighted in purple. At their extreme C-termini both the proteins possess a di-leucine (LL) motif highlighted in blue, and a class II PBM highlighted in green. The tyrosine-based sorting motif (YXXΦ) and the Src Homology 3 (SH3) domain binding motif (PXXP) present in the cytoplasmic domain of CR1β are highlighted in red and brown, respectively.

3.2. HAdV-3 E3-CR1β and E3-CR1γ are expressed predominantly at late times post-infection and co-localize at the plasma membrane of non-polarized epithelial cells

To analyze the kinetics of expression and the subcellular localization of E3-20.1K (E3-CR1β) and E3-20.5K (E3-CR1γ), A549 cells were infected with HAdV-3 N-tag wt at a MOI of 10 pfu/cell. At various times pi total RNA was extracted to investigate the presence of E3-20.1K and E3-20.5K-containing transcripts by end point PCR (Fig. 3A), infected cells lysates were examined by WB analysis (Fig. 3B) or infected cell monolayers on coverslips were fixed and stained for immunofluorescence microspcopy (Fig. 4). E3-20.1K and E3-20.5K transcripts were detected using two different sets of primers that distinguish early transcripts from MLP transcripts. E3-20.1K and E3-20.5K transcripts were detectable as early as 6 hpi and were abundantly produced at late times pi, as MLP transcripts carrying the TPL sequence at their 5' end

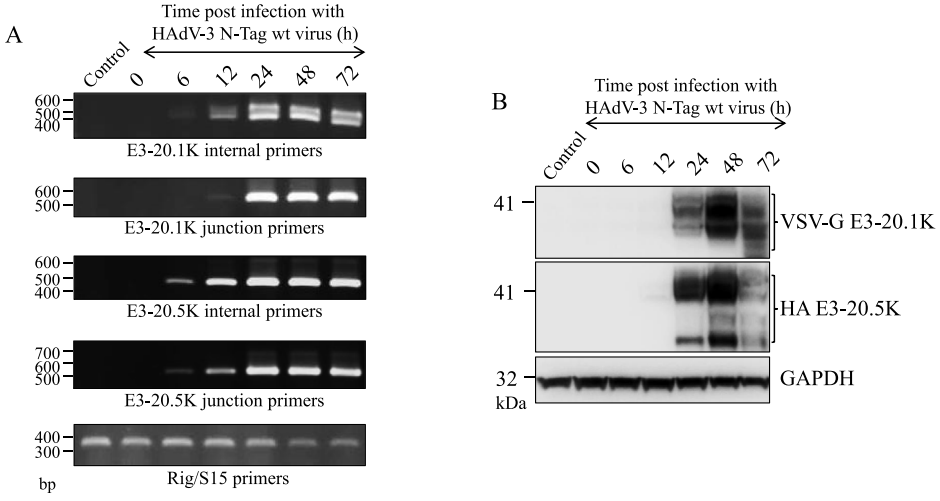

Fig. 3. Time line of HAdV-3 E3-20.1K and E3-20.5K expression in infected A549 cells. A549 cells were infected with HAdV-3 N-tag wt at a MOI of 10 pfu/cell. At indicated times post infection A) total RNA was extracted and reverse transcribed to cDNA. Internal and junction primers were used to detect E3-20.1K and E3-20.5K early and late transcripts. The gel image is representative of three independent experiments. B) the presence of E3-20.1K and E3-20.5K proteins in infected cell lysates was investigated by WB analysis using primary antibodies specific to VSV-G and HA tags, respectively. GAPDH was detected as a loading control. The blot is representative of three independent experiments.

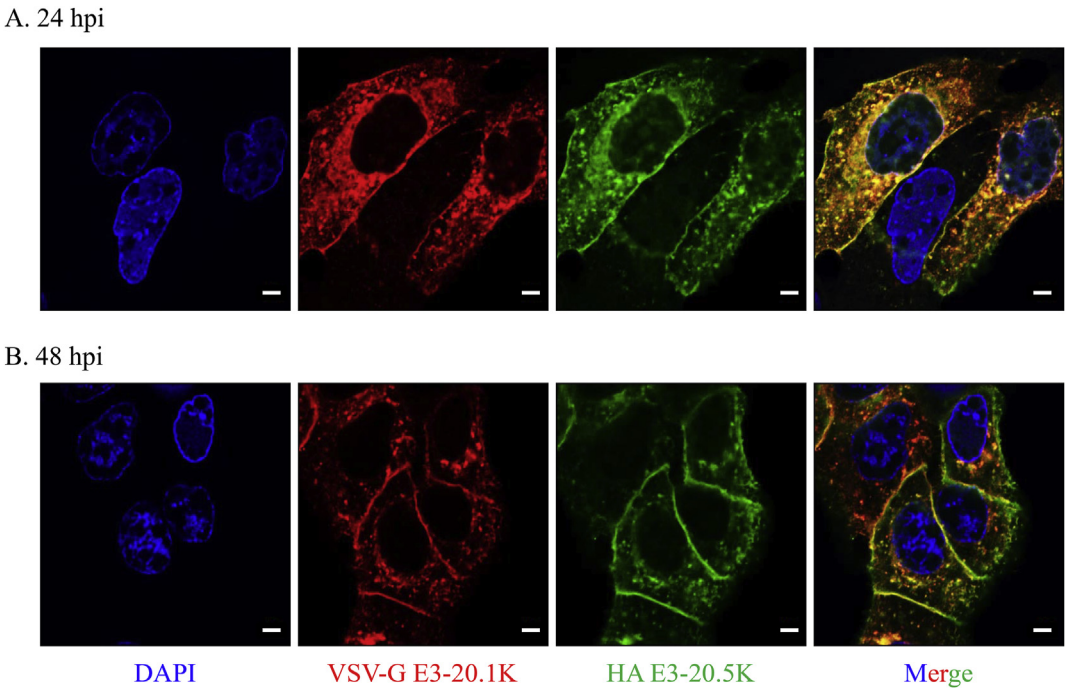

Fig. 4. HAdV-3 E3-20.1K and E3-20.5K proteins co-localize at the plasma membrane in non-polarized A549 cells. A549 cells were infected with the HAdV-3 N-tag wt virus at a MOI of 10 pfu/cell. At A) 24 and B) 48 hpi cell monolayers were fixed for immunofluorescence staining. E3-20.1K and E3-20.5K proteins were detected using primary antibodies specific to VSV-G and HA tags, respectively. Cells were imaged with a Zeiss LSM 8000 AiryScan confocal microscope using a 63X objective. Nuclei were stained with DAPI. Scale bar = 10μM. The images are representative of three independent experiments.

(Fig. 3A). To validate these observations we performed quantitative PCR and readily detected E3-20.1K and E3-20.5K MLP transcripts by 24 hpi (Fig. S5). Expression of both E3-20.1K and E3-20.5K proteins was detectable at 12 hpi, peaked at 48 hpi, and decreased by 72 hpi (Fig. 3B). Immunofluorescence microscopy studies revealed that at 24 hpi both E3-20.1K and E3-20.5K predominantly co-localized to cytoplasmic vesicles and to a lesser extent at the plasma membrane (Fig. 4A). In an attempt to define the identity of the cytoplasmic vesicles, we performed co-localization studies using antibodies specific to PDI, an endoplasmic reticulum (ER) marker, Golgin-97, a trans-Golgi network (TGN) marker, EEA1, an early lysosome marker, and LAMP2, a late endosome/lysosome marker. We observed that at 24 hpi both E3-20.1K and E3-20.5K were present in the ER, TGN, and in early endosomes but not in late endosomes/lysosomes (Figs. S6 and S7, Panels A to D). At 48 hpi when the levels of expression of both proteins peaked, the two E3 proteins co-localized predominantly at the plasma membrane (Fig. 4B). The localization of E3-20.1K and E3-20.5K to the plasma membrane was confirmed by detection of co-localization of the two proteins with E-cadherin (Figs. S6 and S7, Panel E). To validate our observations of subcellular localization, we co-transfected pMT2-PL mammalian expression vectors encoding VSV-G E3-20.1K and HA E3-20.5K (Fig. S3A) into HEK 293T cells. Consistent with the observations in infected A549 cells, both E3-20.1K and E3-20.5K co-localized predominantly to the plasma membrane of transfected HEK 293T cells (Fig. S8).

3.3. HAdV-3 E3-20.1K and E3-20.5K are integral membrane proteins with an N-lumenal and C-cytoplasmic topology

To confirm the predicted topology of HAdV-3 E3-E3-20.1K and E3-20.5K, we generated pMT2-PL mammalian expression vectors encoding either N-terminally tagged or C-terminally tagged full length E3-20.1K and E3-20.5K as shown in the schematic in Figs. S3A and S3B. HEK 293T cells were transfected with N- or C-terminally tagged E3-20.1K and N- or C-terminally tagged E3-20.5K individually and processed for immunofluorescence microscopy at 72 hpt. During the immunostaining procedure, cells were either permeabilized with Triton X-100 or not permeabilized. Consistent with the predictions, N-tagged E3-20.1K and E3-20.5K proteins were detected at the plasma membrane of transfected cells irrespective of whether the cells had been permeabilized or not, while the C-tagged E3-20.1K and E3-20.5K proteins were detected only when the cells were permeabilized (Fig. 5).

We next sought to investigate if any of the identified functional domains/motifs common to E3-20.1K and E3-20.5K were required for the proper localization and orientation of these proteins at the plasma membrane. We generated pMT2-PL or pMEGFP-C1 mammalian expression constructs carrying deletion mutants of E3-20.1K and E3-20.5K lacking the N-terminal or C-terminal domain, with or without TM domains as shown in the schematic in Fig. S3. In addition, we either mutated or deleted the predicted functional motifs identified in the cytoplasmic tail of E3-20.1K and E3-20.5K. HEK 293T cells were transfected with these different constructs. As shown in Fig. 6, obliteration of the di-leucine motifs (LL/AA mutant) or deletion of the class II PBM (ΔPBM mutant) did not alter the localization of E3-20.1K or E3-20.5K (Fig. 6A, 6B, and 6C). In the absence of the TM domain, small peptides representing the N-terminal or the C-terminal domains of E3-20.1K and E3-20.5K localized to the nucleus and/or to the cytoplasm of transfected cells (Fig. 6D and 6F). However, the presence of the TM domain was sufficient to direct both N-terminal and C-terminal domains of E3-20.1K and E3-20.5K to the plasma membrane (Fig. 6E and 6G).

3.4. HAdV-3 E3-20.1K is N-glycosylated while E3-20.5K is O- and N-glycosylated

The glycosylation state of E3-20.1K and E3-20.5K was examined in A549 cells infected with HAdV-3 N-tag wt at a MOI of 10 pfu/cell. At 48 hpi cell lysates were treated with PNGase F, α2-3,6,8,9 neuraminidase A, and O-glycosidase either individually or sequentially (Fig. 7). Untreated E3-20.1K migrates at approximately 40 kDa. Treatment with PNGase F resulted in an electrophoretic mobility shift to approximately 20 kDa, the predicted size of the translationally unmodified

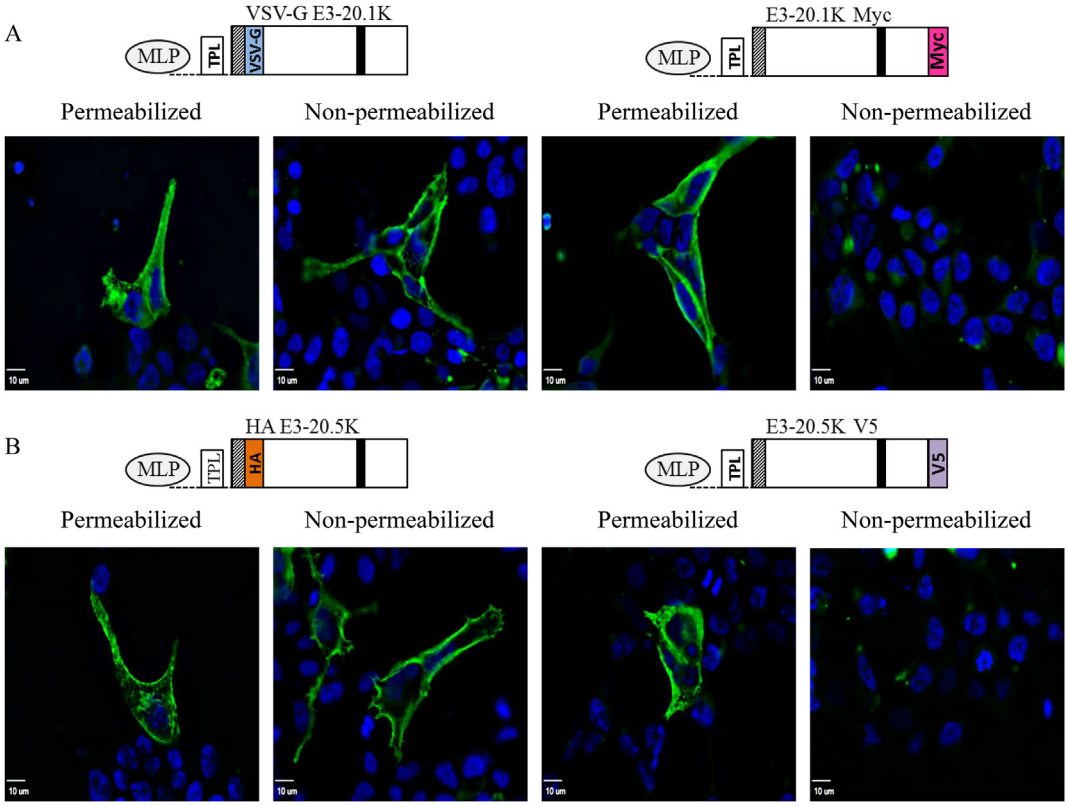

Fig. 5. HAdV-3 E3-20.1K and E3-20.5K are type I integral membrane proteins with N-luminal and C-cytoplasmic topology. pMT2-PL mammalian expression vectors encoding N- or C-terminally tagged A) E3-20.1K and B) E3-20.5K under the control of the HAdV-C2 derived major late promoter (MLP) were transfected into HEK 293T cells. At 72 hpt cell monolayers were fixed for immunofluorescence staining. During the staining procedure cells were either not permeabilized, or permeabilized with 0.5% Triton X-100 as indicated. The cells were stained with the primary antibody targeting the small epitope tag (green). Nuclei were stained with DAPI (blue). Images were acquired at 63x magnification using a Zeiss Axioskop epifluorescence microscope. TPL: Tri partite leader sequence. The images are representative of at least 20 fields analyzed from two independent experiments.

polypeptide, indicating the presence of N-glycosylation. Treatment with α2-3,6,8,9 neuraminidase A and O-glycosidase either individually or sequentially did not change the electrophoretic mobility of E3-20.1K. However, sequential treatment with PNGase F, α2-3,6,8,9 neuraminidase A, and O-glycosidase resulted in the migration of E3-20.1K at approximately 20 kDa, like after PNGase F treatment (Fig. 7) indicating that E3-20.1K is N- but not O-glycosylated. Untreated E3-20.5K migrated at approximately 40 and 25 kDa, likely as a result of differential glycosylation or partial glycosylation. Treatment with PNGase F resulted in a mobility shift of both bands to approximately 35 kDa and 20 kDa, respectively indicating presence of N-glycosylation. The 20 kDa band represents the predicted size of the translationally unmodified E3-20.5K polypeptide. Treatment with α2-3,6,8,9 neuraminidase A individually, or sequential treatment with α2-3,6,8,9 neuraminidase A and O-glycosidase resulted in the mobility shift of the 40 kDa band only, without affecting the 25 kDa band. However, sequential treatment with PNGase F, α2-3,6,8,9 neuraminidase A, and O-glycosidase resulted in complete deglycosylation and migration of both bands at approximately 20 kDa (Fig. 7). This result is in agreement with that reported by Hawkins and colleagues (Hawkins and Wold, 1995) and shows that E3-20.5 K is both N- and O-glycosylated.

3.5. HAdV-3 E3-20.1K and E3-20.5K interact with each other

The observation of co-localization of E3-20.1K and E3-20.5K at the plasma membrane in infected/transfected cells prompted us to examine whether these proteins physically interact with each other. HEK 293T cells were transfected with pMT2-PL mammalian expression vectors encoding VSV-G E3-20.1K and HA E3-20.5K either individually or together. At 72 hpt, cells were lysed and immunoprecipitated with antibodies specific to either VSV-G or HA to pull down E3-20.1K or E3-20.5K, respectively. The immunoprecipitated proteins were analyzed by WB to evaluate if VSV-G E3-20.1K pulled down HA E3-20.5K and vice versa. Fig. 8 shows that VSV-G E3-20.1K and HA E3-20.5K co-immunoprecipitated with each other indicating that the two proteins do interact.

3.6. E3-20.1K and E3-20.5K do not appear to play a role in HAdV-3 progeny release and in HAdV-3 spread in A549 cells

We next examined the role of HAdV-3 E3-20.1K and E3-20.5K in virus progeny release from infected A549 cells. We generated a double knock out virus (HAdV-3 N-tag DKO) that does not express E3-20.1K and E3-20.5K proteins (Figs. S2A and S2B). A549 cells were infected with HAdV-3 wt, HAdV-3 N-tag wt or, HAdV-3 N-tag DKO mutant virus at a MOI of 1 pfu/cell. At different times pi the extracellular compartment (supernatant) (Fig. 9A) or whole dish contents (total virus: cell monolayer and supernatant) (Fig. 9B) were sampled to determine infectious virus loads. We observed no difference in infectious virus titers in either the extracellular compartment or in the total virus yields between cells infected with HAdV-3 wt, HAdV-3 N-tag wt, or HAdV-3 N-tag DKO. The contribution of E3-20.1K and E3-20.5K to HAdV-3 spread in cell culture was evaluated using a dissemination assay and by examination of plaque phenotypes. We observed no differences in viral spread phenotype (Fig. 9C), or in plaque size and morphology (Fig. S9) between wt and DKO-infected cells.

4. Discussion

This body of work provides a foundational characterization of

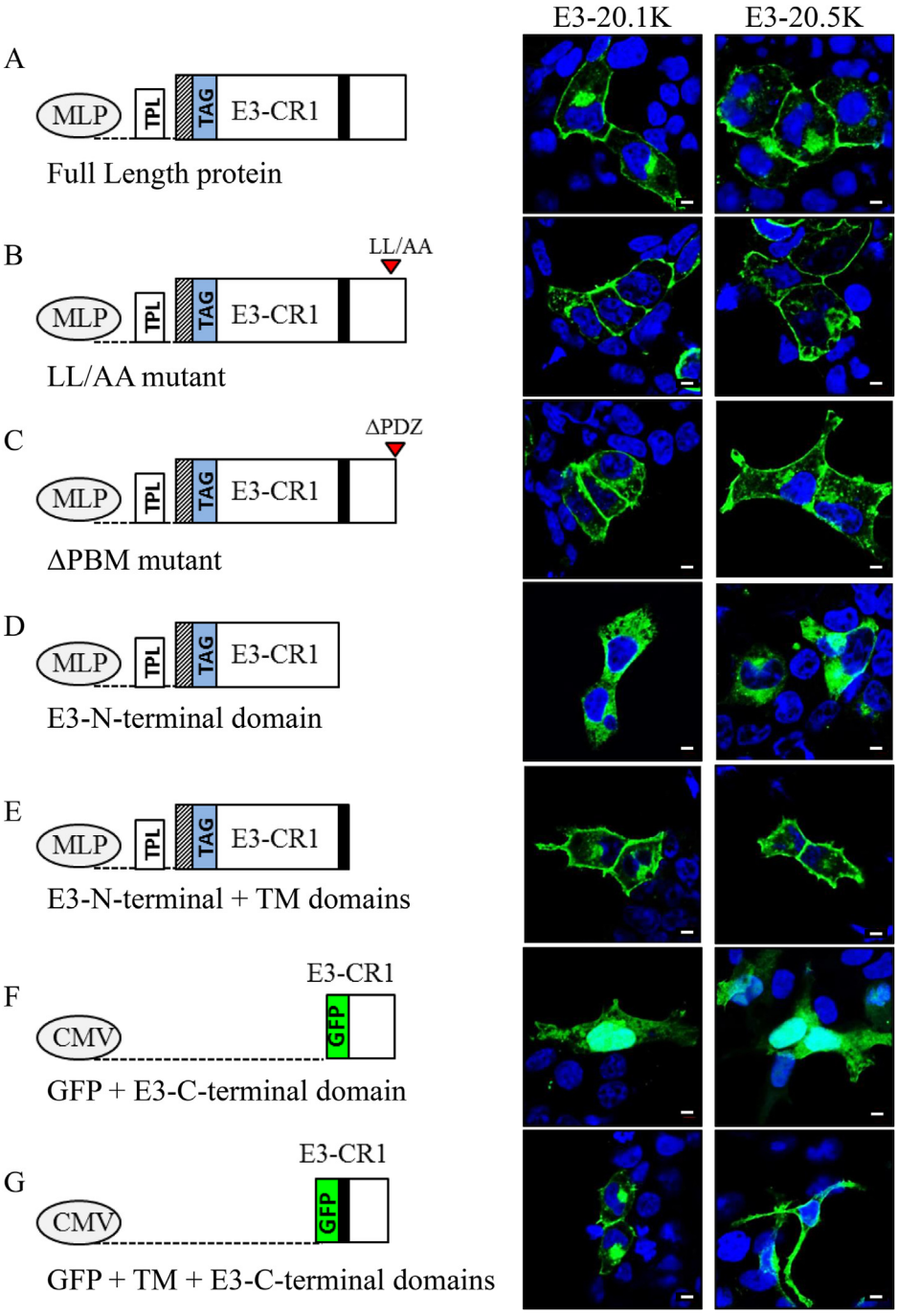

Fig. 6. The transmembrane domains of E3-20.1K and E3-20.5K are essential for their proper localization at the plasma membrane. HEK 293T cells were transfected with pMT2-PL mammalian expression vectors encoding A) N-terminally tagged full length E3-20.1K and E3-20.5K proteins. B) E3-20.1K and E3-20.5K LL/AA mutants that have the di-leucine motif mutated to two alanine amino acid residues. C) E3-20.1K and E3-20.5K ΔPBM mutants that lack the 4 amino acids at the extreme C-terminus; D) and E) the N-terminal domain of E3-20.1K and E3-20.5K without or with the TM domain; F) and G) pMEGFP vector encoding the C-terminal domain of E3-20.1K and E3-20.5K without or with the TM domain. At 72 h post transfection the cells were fixed for immunofluorescence staining with specific anti tag antibodies (green) or directly mounted in the case of cells transfected with constructs expressing GFP fusion proteins. Images were acquired at 63x magnification using a Zeiss LSM 8000 AiryScan confocal microscope. Bar = 10μM. Nuclei (Blue). The images are representative of at least 20 fields analyzed from two independent experiments.

HAdV-3-encoded E3-CR1β and E3-CR1γ. These HAdV-B-specific E3-CR1 proteins are conserved among human and simian types and present in all examined genomes indicating that they are highly likely to contribute to virus-host interactions occurring during infection. In infected A549 cells the two proteins were readily detectable at late times post infection, presumably as a result of translation of MLP transcripts. The results of our recent studies determining the critical contribution of the TPL sequence to the successful ectopic expression of HAdV-B and HAdV-E E3 CR1 genes (Bair et al., 2017) suggest that the presence of this non-coding element is essential for efficient translation of HAdV-3 E3-20.1K and E3-20.5K transcripts at late times post infection.

Our data show that E3-20.1K is only N-glycosylated while, as previously reported by Hawkins and Wold (1995), HAdV-3 E3-20.5K is both N- and O-glycosylated. We also conclusively demonstrate that E3-20.1K and E3-20.5K are type I transmembrane proteins that co-localize predominantly to the cytoplasmic vesicles at 24 hpi and to the plasma membrane at 48 hpi in non-polarized epithelial cells (A549 and HEK 293Ts).

A thorough examination of the subcellular localization of these proteins by confocal fluorescence microscopy at 24 hpi revealed that at steady-state both proteins localize to the ER, TGN, and early endosomes but not to the late endosomes/lysosomes. These results suggest that E3-20.1K and E3-20.5K traffic to the plasma membrane along the secretory pathway. Interestingly, we observed that a considerable proportion of the detectable E3-20.1K and E3-20.5K at 24 hpi localized to cytoplasmic vesicles that could not be identified by our efforts. This suggests that the proteins may be delivered to the plasma membrane by secretory vesicles or by unconventional pathways including secretory autophagy (Cotzomi-Ortega et al., 2018) warranting additional studies using an expanded panel of markers. The fact that E3-20.1K and E3-

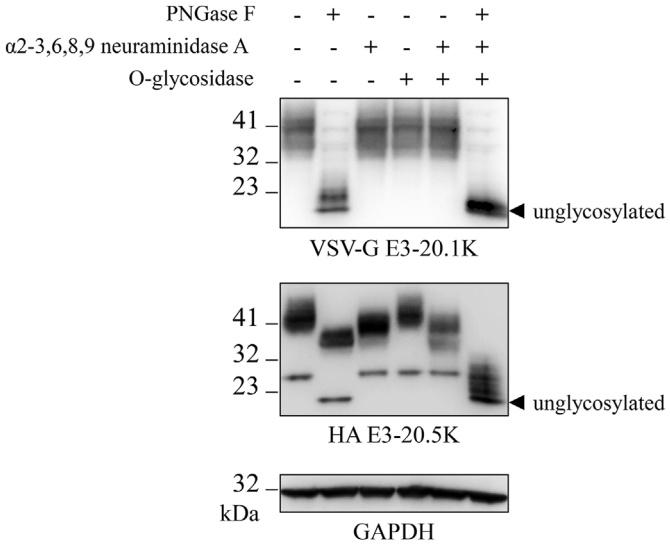

Fig. 7. HAdV-3 E3-20.1K is N-glycosylated whereas E3-20.5K is N-and O-glycosylated. A549 cells were infected with the HAdV-3 N-tag wt virus at a MOI of 10 pfu/cell. At 48 hpi cell lysates were prepared and treated for 1 h with PNGase F, or α2-3,6,8,9 neuraminidase A, or O-glycosidase either individually or sequentially with α2-3,6,8,9 neuraminidase A and o-glycosidase or with PNGase F, α2-3,6,8,9 neuraminidase A, and o-glycosidase in the order mentioned. After treatment, the lysates were analyzed for the expression of VSV-G E3-20.1K, HA E3-20.5K, and GAPDH (loading control) by SDS-PAGE and WB. The blot is representative of three independent experiments.

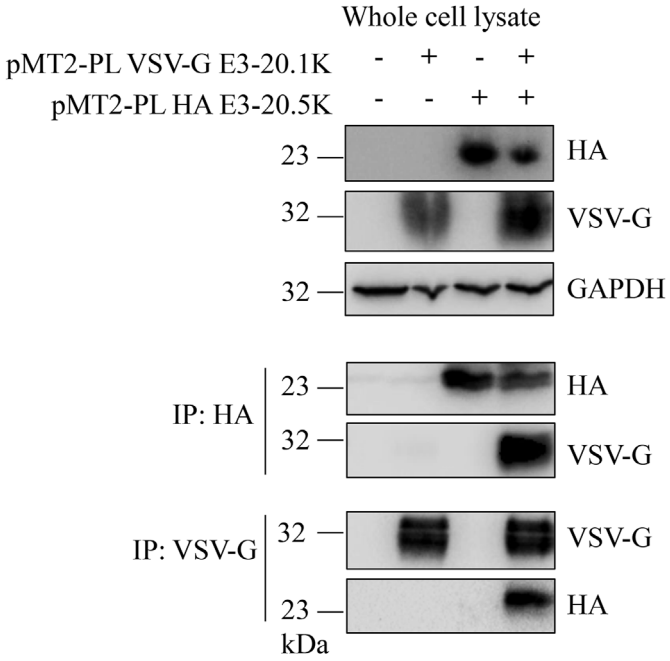

Fig. 8. HAdV-3 E3-20.1K and E3-20.5K interact with each other. pMT2-PL constructs encoding VSV-G E3-20.1K and HA E3-20.5K were transfected into HEK 293T cells either individually or together. At 72 h post transfection, total cell lysates were analyzed by WB for expression of E3-20.1K and E3-20.5K with anti-tag antibodies. Additionally, the lysates were subjected to immunoprecipitation with anti VSV-G or anti HA conjugated magnetic beads to pull down E3-20.1K or E3-20.5K respectively. Pulled down samples were analyzed by WB for the presence of E3-20.5K or E3-20.1K, respectively. The blot is representative of three independent experiments.

20.5K co-immunoprecipitate suggests that these proteins may work together to carry out their biological functions.

In a recent study of the HAdV E3-CR1 host extracellular interactome using C-terminal IgG Fc fusion of the E3 CR1 protein ectodomains as baits and an extracellular protein microarray, Martinez Martin and colleagues demonstrated that the N-terminal domain of HAdV-B E3-CR1β interacts with the signaling lymphocyte activation molecule (SLAM) family of receptors and inhibits T-cell activation. The N-terminal domain of HAdV-B E3-CR1γ was also shown to interact with SLAM receptors, although the functional implications of this interaction were not investigated (Martinez-Martin et al., 2016). Our study shows that the C-termini of both E3-20.1K and E3-20.5K have a class II PBM suggesting that these proteins may carry out additional functions within the host cell through interactions with PDZ proteins. Multiple sequence analysis indicates that the class II PBM is conserved among the E3-CR1β and E3-CR1γ proteins of all of simian and human members of species HAdV-B.

The LL motif was found in all of the examined HAdV-B E3-CR1β and E3-CR1γ proteins. The YXXΦ motif is present in all of the E3-CR1β proteins encoded by human types and in most of the E3-CR1β proteins encoded by simian members of the species. Interestingly, while the YXXΦ motif is also present in many of the E3-CR1γ proteins encoded by simian HAdV-B, it is not present in any of the E3-CR1γ encoded by human types classified within this species. The LL and YXXΦ motifs are sorting signals that aid in the trafficking of proteins through the secretory pathway and in the targeting of membrane proteins to the basolateral surface of polarized epithelial cells (Heilker et al., 1999; Miranda et al., 2001). Like the LL motif in HAdV-D-specific E3-49K, the LL motif in HAdV-B E3-CR1β and E3-CR1γ does not fit the consensus sequence of acidic (D/E)*XXX*L(L/I) or D*XX*LL di-leucine motifs (Windheim et al., 2016). The LL motif of HAdV-D E3-49K was shown to be important for trafficking of the full length protein and the C-terminal portion of the cleaved protein from the cell surface to the early endosome/trans Golgi network (TGN) and lysosomes, respectively (Windheim et al., 2016). Our observations of subcellular localization of ectopically-expressed mutant versions of HAdV-3 E3-20.1K and E3-20.5K indicate that, at least in our experimental system, obliteration of the LL motif or deletion of the class II PBM did not affect the localization of these proteins to the plasma membrane. Likewise, deletion of the N-terminal or C-terminal domains while retaining the transmembrane domain did not alter the localization of E3-20.1K and E3-20.5K. These results indicate that the TM domain of these proteins is sufficient for localization to the plasma membrane and that neither the LL nor the class II PBM nor the YXXΦ motifs play a critical role in their trafficking to the plasma membrane in non-polarized cells.

The presence of a class II PBMs in the extreme C-termini of HAdV-B E3-CR1β and E3-CR1γ has not been previously reported. The identified PBMs have the typical 4-amino acid length and the localization described for PBMs in general and are therefore anticipated to be functional (Hung and Sheng, 2002; Nourry et al., 2003). The PBM has the potential to confer these HAdV-B-specific E3-CR1 proteins the ability to interact with PDZ-domain containing host proteins and therefore deserves further investigation for elucidation of functional implications. Our thorough examination of E3-CR1 protein sequences for a wide range of HAdV types representing species HAdV-A through -G identified a putative class II PBM (-SLTV$_{COOH}$), at the extreme C-terminus of E3-CR1β/11.6K encoded by various strains of HAdV-C5 (AC_000008, AY601635, KX868466, KF429754, MF681662 among others) but intriguingly, not by E3-CR1β/11.6K of types HAdV-C1, -C2 and –C6 (data not shown). We also observed that the C-termini of E3-CR1α proteins encoded by HAdV-D8 (AB448769), -D9 (AJ854486), -D15 (AB562586), -D19 (AB448774), -D37 (AB448778), -D46 (AY875648), -D56 (HM770721), and -D64 (EF121005) possess a class III PBM (consensus sequence (D/E)XΦ, where X = any amino acid, and Φ = hydrophobic amino acid) (data not shown).

In humans, PDZ domains are found in over 200 proteins that primarily contribute to the generation and maintenance of cell-cell junctions and cell polarity, or that are involved in cellular signal transduction pathways. (Assemat et al., 2008; Spaller, 2006). Several viral

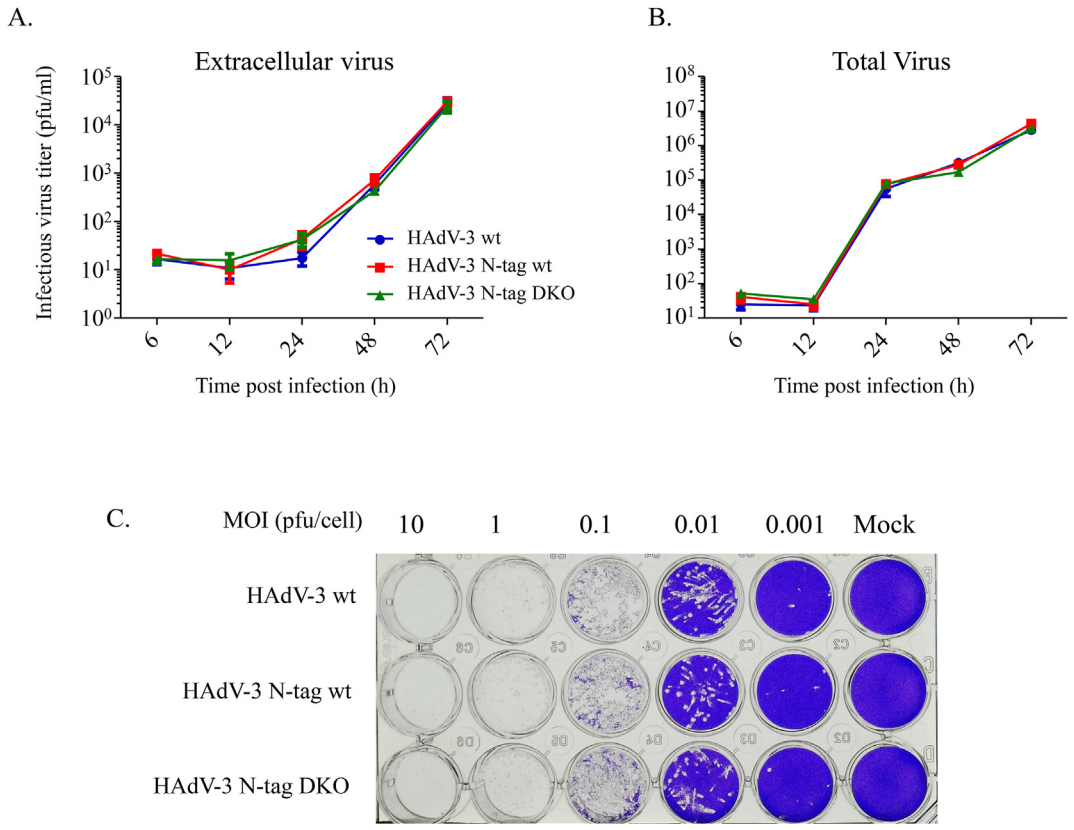

Fig. 9. HAdV-3 E3-20.1K and E3-20.5K do not appear to contribute to viral progeny release or viral spread in infected A549 cells. A549 cells were infected with HAdV-3 wt, HAdV-3 N-tag wt, or HAdV-3 N-tag DKO mutant virus at a MOI of 1 pfu/cell. At indicated times post infection A) extracellular or B) total (intracellular and extracellular) infectious virus titers were determined by plaque assay to assess the kinetics of virus progeny release. Error bars represent the standard error of the mean from 3 biological replicates assayed in duplicate. C) A549 cells were infected with HAdV-3 wt, N-tag wt, or N-tag DKO mutant at various MOIs ranging from 10 to 0.001 pfu/cell. At 7 dpi, cells were fixed and stained to visualize virus dissemination. The data are representative of three independent experiments.

proteins are known to encode PBMs that target host PDZ domain-containing proteins to modulate cellular processes in support of virus replication, viral pathogenesis, and virus dissemination or transmission to new host (Javier and Rice, 2011). For example, adenovirus E4-ORF1 contains a class I PBM (-ATLV$_{COOH}$) through which E4-ORF1 binds PDZ domain containing proteins to disrupt epithelial cell junctions of infected cells (Latorre et al., 2005). The SARS coronavirus envelope protein E contains a Class II PBM (-DLLV$_{COOH}$) that mediates the interaction of the protein with PALS1, affecting tight junction formation in infected cells (Teoh et al., 2010).

Our results show that unlike the HAdV-C-specific E3-CR1β/ADP (Tollefson et al., 1996a, 1996b), HAdV-3-encoded E3-CR1β and E3-CR1γ do not play a role in virus progeny release, cell-to-cell spread or plaque formation in non-polarized cells. However, the subcellular localization of E3-CR1β and E3-CR1γ as well as their contribution to virus progeny release and their effect on epithelial barrier integrity should be re-examined in polarized epithelial cells. By using our HAdV-3 mutants in a more physiologically relevant experimental system, the role of these two CR1 proteins during the HAdV-B's life cycle may be more easily unveiled and protein-protein interactions more accurately localized to specific cellular domains.

The Syrian hamster recently shown by Radke and colleagues (Radke et al., 2016) to support replication of HAdV-14, a member of species HAdV-B, is an interesting animal model to be considered for the examination of the role of E3-CR1β and E3-CR1γ during infection *in vivo*. The detection of HAdV-14 hexon protein in the lungs of infected hamsters suggests that E3-CR1 proteins would be expressed at detectable levels in this host, opening new opportunities for viral pathogenesis studies.

CRediT authorship contribution statement

Poornima Kotha Lakshmi Narayan: Methodology, Investigation, Formal analysis, Data curation, Writing - original draft, Writing - review & editing. **Adriana E. Kajon:** Funding acquisition, Supervision, Conceptualization, Formal analysis, Data curation, Writing - original draft, Writing - review & editing.

Declaration of competing interest

The authors declare no conflict of interest.

Acknowledgements

We would like to thank Dr. Silvio Hemi for the kind gift of pKSB2Ad3wt bacmid, and Anjinette R. Lewis for her assistance with the construction of mammalian expression vectors encoding mutant E3-20.1K and E3-20.5K. This research made use of the Fluorescence Microscopy and Cell Imaging shared resource supported by the University of New Mexico Comprehensive Cancer Center Support Grant NCI P30CA118100.

Appendix A. Supplementary data

Supplementary data to this article can be found online at https://doi.org/10.1016/j.virol.2020.04.005.

Funding source

Lovelace Respiratory Research Institute intramural support to AEK.

References

Assemat, E., Bazellieres, E., Pallesi-Pocachard, E., Le Bivic, A., Massey-Harroche, D., 2008. Polarity complex proteins. Biochim. Biophys. Acta 1778, 614–630.
Bair, C.R., Kotha Lakshmi Narayan, P., Kajon, A.E., 2017. The tripartite leader sequence is required for ectopic expression of HAdV-B and HAdV-E E3 CR1 genes. Virology 505, 139–147.
Benedict, C.A., Norris, P.S., Prigozy, T.I., Bodmer, J.L., Mahr, J.A., Garnett, C.T., Martinon, F., Tschopp, J., Gooding, L.R., Ware, C.F., 2001. Three adenovirus E3 proteins cooperate to evade apoptosis by tumor necrosis factor-related apoptosis-inducing ligand receptor-1 and -2. J. Biol. Chem. 276, 3270–3278.
Brown, R.S., Nogrady, M.B., Spence, L., Wiglesworth, F.W., 1973. An outbreak of adenovirus type 7 infection in children in Montreal. Can. Med. Assoc. J. 108, 434–439.
Burgert, H.G., Blusch, J.H., 2000. Immunomodulatory functions encoded by the E3 transcription unit of adenoviruses. Virus Gene. 21, 13–25.
Burgert, H.G., Kvist, S., 1985. An adenovirus type 2 glycoprotein blocks cell surface expression of human histocompatibility class I antigens. Cell 41, 987–997.
Chen, M., Zhu, Z., Huang, F., Liu, D., Zhang, T., Ying, D., Wu, J., Xu, W., 2015. Adenoviruses associated with acute respiratory diseases reported in Beijing from 2011 to 2013. PloS One 10, e0121375.
Cheng, Z., Yan, Y., Jing, S., Li, W.G., Chen, W.W., Zhang, J., Li, M., Zhao, S., Cao, N., Ou, J., Zhao, S., Wu, X., Cao, B., Zhang, Q., 2018. Comparative genomic analysis of Re-emergent human adenovirus type 55 pathogens associated with adult severe community-acquired pneumonia reveals conserved genomes and capsid proteins. Front. Microbiol. 9, 1180.
Chia, S.L., Lei, J., Ferguson, D.J.P., Dyer, A., Fisher, K.D., Seymour, L.W., 2017. Group B adenovirus enadenotucirev infects polarised colorectal cancer cells efficiently from the basolateral surface expected to be encountered during intravenous delivery to treat disseminated cancer. Virology 505, 162–171.
Cotzomi-Ortega, I., Aguilar-Alonso, P., Reyes-Leyva, J., Maycotte, P., 2018. Autophagy and its role in protein secretion: implications for cancer therapy. Mediat. Inflamm. 4231591 2018.
Cui, X., Wen, L., Wu, Z., Liu, N., Yang, C., Liu, W., Ba, Z., Wang, J., Yi, S., Li, H., Liang, B., Li, P., Jia, L., Hao, R., Wang, L., Hua, Y., Wang, Y., Qiu, S., Song, H., 2015. Human adenovirus type 7 infection associated with severe and fatal acute lower respiratory illness and nosocomial transmission. J. Clin. Microbiol. 53, 746–749.
Davison, A.J., Akter, P., Cunningham, C., Dolan, A., Addison, C., Dargan, D.J., Hassan-Walker, A.F., Emery, V.C., Griffiths, P.D., Wilkinson, G.W., 2003a. Homology between the human cytomegalovirus RL11 gene family and human adenovirus E3 genes. J. Gen.Virol. 84, 657–663.
Davison, A.J., Benko, M., Harrach, B., 2003b. Genetic content and evolution of adenoviruses. J. Gen.Virol. 84, 2895–2908.
Doronin, K., Toth, K., Kuppuswamy, M., Krajcsi, P., Tollefson, A.E., Wold, W.S., 2003. Overexpression of the ADP (E3-11.6K) protein increases cell lysis and spread of adenovirus. Virology 305, 378–387.
Echavarria, M., 2008. Adenoviruses in immunocompromised hosts. Clin. Microbiol. Rev. 21, 704–715.
Espinola, E.E., Barrios, J.C., Russomando, G., Mirazo, S., Arbiza, J., 2017. Computational analysis of a species D human adenovirus provides evidence of a novel virus. J. Gen.Virol. 98, 2810–2820.
Frietze, K.M., Campos, S.K., Kajon, A.E., 2010. Open reading frame E3-10.9K of subspecies B1 human adenoviruses encodes a family of late orthologous proteins that vary in their predicted structural features and subcellular localization. J. Virol. 84, 11310–11322.
Gooding, L.R., Elmore, L.W., Tollefson, A.E., Brady, H.A., Wold, W.S., 1988. A 14,700 MW protein from the E3 region of adenovirus inhibits cytolysis by tumor necrosis factor. Cell 53, 341–346.
Gopalkrishna, V., Ganorkar, N.N., Patil, P.R., 2016. Identification and molecular characterization of adenovirus types (HAdV-8, HAdV-37, HAdV-4, HAdV-3) in an epidemic of keratoconjunctivitis occurred in Pune, Maharashtra, Western India. J. Med. Virol. 88, 2100–2105.
Guo, D.F., Shinagawa, M., Aoki, K., Sawada, H., Itakura, S., Sato, G., 1988. Genome typing of adenovirus strains isolated from conjunctivitis in Japan, Australia, and the Philippines. Microbiol. Immunol. 32, 1107–1118.
Hage, E., Huzly, D., Ganzenmueller, T., Beck, R., Schulz, T.F., Heim, A., 2014. A human adenovirus species B subtype 21a associated with severe pneumonia. J. Infect. 69, 490–499.
Hawkins, L.K., Wold, W.S., 1995. The E3-20.5K membrane protein of subgroup B human adenoviruses contains O-linked and complex N-linked oligosaccharides. Virology 210, 335–344.
Heilker, R., Spiess, M., Crottet, P., 1999. Recognition of sorting signals by clathrin adaptors. Bioessays : news and reviews in molecular, cellular and developmental biology 21, 558–567.
Hemminki, O., Bauerschmitz, G., Hemmi, S., Lavilla-Alonso, S., Diaconu, I., Guse, K., Koski, A., Desmond, R.A., Lappalainen, M., Kanerva, A., Cerullo, V., Pesonen, S., Hemminki, A., 2011. Oncolytic adenovirus based on serotype 3. Canc. Gene Ther. 18, 288–296.
Hofland, C.A., Eron, L.J., Washecka, R.M., 2004. Hemorrhagic adenovirus cystitis after renal transplantation. Transplant. Proc. 36, 3025–3027.
Houldcroft, C.J., Beale, M.A., Sayeed, M.A., Qadri, F., Dougan, G., Mutreja, A., 2018. Identification of novel adenovirus genotype 90 in children from Bangladesh. Microb. Genom. 4, e000221.
Hung, A.Y., Sheng, M., 2002. PDZ domains: structural modules for protein complex assembly. J. Biol. Chem. 277, 5699–5702.
Javier, R.T., Rice, A.P., 2011. Emerging theme: cellular PDZ proteins as common targets of pathogenic viruses. J. Virol. 85, 11544–11556.
Kajon, A.E., Erdman, D.D., 2007. Assessment of genetic variability among subspecies b1 human adenoviruses for molecular epidemiology studies. Methods Mol. Med. 131, 335–355.
Kajon, A.E., Ison, M.G., 2016. Severe infections with human adenovirus 7d in 2 adults in family, Illinois, USA, 2014. Emerg. Infect. Dis. 22, 730–733.
Kajon, A.E., Lamson, D.M., St George, K., 2019. Emergence and re-emergence of respiratory adenoviruses in the United States. Current opinion in virology 34, 63–69.
Kajon, A.E., Lu, X., Erdman, D.D., Louie, J., Schnurr, D., George, K.S., Koopmans, M.P., Allibhai, T., Metzgar, D., 2010. Molecular epidemiology and brief history of emerging adenovirus 14-associated respiratory disease in the United States. J. Infect. Dis. 202, 93–103.
Kajon, A.E., Xu, W., Erdman, D.D., 2005. Sequence polymorphism in the E3 7.7K ORF of subspecies B1 human adenoviruses. Virus Res. 107, 11–19.
Keller, E.W., Rubin, R.H., Black, P.H., Hirsch, M.S., Hierholzer, J.C., 1977. Isolation of adenovirus type 34 from a renal transplant recipient with interstitial pneumonia. Transplantation 23, 188–191.
Khan, S., Oosterhuis, K., Wunderlich, K., Bunnik, E.M., Bhaggoe, M., Boedhoe, S., Karia, S., Steenbergen, R.D.M., Bosch, L., Serroyen, J., Janssen, S., Schuitemaker, H., Vellinga, J., Scheper, G., Zahn, R., Custers, J., 2017. Development of a replication-deficient adenoviral vector-based vaccine candidate for the interception of HPV16- and HPV18-induced infections and disease. Int. J. Canc. 141, 393–404.
Latorre, I.J., Roh, M.H., Frese, K.K., Weiss, R.S., Margolis, B., Javier, R.T., 2005. Viral oncoprotein-induced mislocalization of select PDZ proteins disrupts tight junctions and causes polarity defects in epithelial cells. J. Cell Sci. 118, 4283–4293.
Li, N., Cooney, A.L., Zhang, W., Ehrhardt, A., Sinn, P.L., 2019. Enhanced tropism of species B1 adenoviral-based vectors for primary human airway epithelial cells. Molecular therapy. Methods & clinical development 14, 228–236.
Lin, Y.C., Lu, P.L., Lin, K.H., Chu, P.Y., Wang, C.F., Lin, J.H., Liu, H.F., 2015. Molecular epidemiology and phylogenetic analysis of human adenovirus caused an outbreak in taiwan during 2011. PloS One 10, e0127377.
Martinez-Martin, N., Ramani, S.R., Hackney, J.A., Tom, I., Wranik, B.J., Chan, M., Wu, J., Paluch, M.T., Takeda, K., Hass, P.E., Clark, H., Gonzalez, L.C., 2016. The extracellular interactome of the human adenovirus family reveals diverse strategies for immunomodulation. Nat. Commun. 7, 11473.
Martone, W.J., Hierholzer, J.C., Keenlyside, R.A., Fraser, D.W., D'Angelo, L.J., Winkler, W.G., 1980. An outbreak of adenovirus type 3 disease at a private recreation center swimming pool. Am. J. Epidemiol. 111, 229–237.
Miranda, K.C., Khromykh, T., Christy, P., Le, T.L., Gottardi, C.J., Yap, A.S., Stow, J.L., Teasdale, R.D., 2001. A dileucine motif targets E-cadherin to the basolateral cell surface in Madin-Darby canine kidney and LLC-PK1 epithelial cells. J. Biol. Chem. 276, 22565–22572.
Nourry, C., Grant, S.G., Borg, J.P., 2003. PDZ Domain Proteins: Plug and Play! Science's STKE : Signal Transduction Knowledge Environment 2003. pp. RE7.
Radke, J.R., Yong, S.L., Cook, J.L., 2016. Low-level expression of the E1B 20-kilodalton protein by adenovirus 14p1 enhances viral immunopathogenesis. J. Virol. 90, 497–505.
Rawle, F.C., Tollefson, A.E., Wold, W.S., Gooding, L.R., 1989. Mouse anti-adenovirus cytotoxic T lymphocytes. Inhibition of lysis by E3 gp19K but not E3 14.7K. J. Immunol. 143, 2031–2037.
Robinson, C.M., Shariati, F., Gillaspy, A.F., Dyer, D.W., Chodosh, J., 2008. Genomic and bioinformatics analysis of human adenovirus type 37: new insights into corneal tropism. BMC Genom. 9, 213.
Seshidhar Reddy, P., Ganesh, S., Limbach, M.P., Brann, T., Pinkstaff, A., Kaloss, M., Kaleko, M., Connelly, S., 2003. Development of adenovirus serotype 35 as a gene transfer vector. Virology 311, 384–393.
Shisler, J., Yang, C., Walter, B., Ware, C.F., Gooding, L.R., 1997. The adenovirus E3-10.4K/14.5K complex mediates loss of cell surface Fas (CD95) and resistance to Fas-induced apoptosis. J. Virol. 71, 8299–8306.
Signas, C., Akusjarvi, G., Pettersson, U., 1986. Region E3 of human adenoviruses; differences between the oncogenic adenovirus-3 and the non-oncogenic adenovirus-2. Gene 50, 173–184.
Siminovich, M., Murtagh, P., 2011. Acute lower respiratory tract infections by adenovirus in children: histopathologic findings in 18 fatal cases. Pediatr. Dev. Pathol. : Off. J.Soc.Pediatr. Pathol.Paediatr. Pathol.Soc. 14, 214–217.
Sirena, D., Ruzsics, Z., Schaffner, W., Greber, U.F., Hemmi, S., 2005. The nucleotide sequence and a first generation gene transfer vector of species B human adenovirus serotype 3. Virology 343, 283–298.
Spaller, M.R., 2006. Act globally, think locally: systems biology addresses the PDZ domain. ACS Chem. Biol. 1, 207–210.
Stalder, H., Hierholzer, J.C., Oxman, M.N., 1977. New human adenovirus (candidate adenovirus type 35) causing fatal disseminated infection in a renal transplant recipient. J. Clin. Microbiol. 6, 257–265.
Stone, D., Ni, S., Li, Z.Y., Gaggar, A., DiPaolo, N., Feng, Q., Sandig, V., Lieber, A., 2005. Development and assessment of human adenovirus type 11 as a gene transfer vector. J. Virol. 79, 5090–5104.
Teoh, K.T., Siu, Y.L., Chan, W.L., Schluter, M.A., Liu, C.J., Peiris, J.S., Bruzzone, R., Margolis, B., Nal, B., 2010. The SARS coronavirus E protein interacts with PALS1 and alters tight junction formation and epithelial morphogenesis. Mol. Biol. Cell 21, 3838–3852.
Tollefson, A.E., Hermiston, T.W., Lichtenstein, D.L., Colle, C.F., Tripp, R.A., Dimitrov, T.,

Toth, K., Wells, C.E., Doherty, P.C., Wold, W.S., 1998. Forced degradation of Fas inhibits apoptosis in adenovirus-infected cells. Nature 392, 726–730.
Tollefson, A.E., Ryerse, J.S., Scaria, A., Hermiston, T.W., Wold, W.S., 1996a. The E3-11.6-kDa adenovirus death protein (ADP) is required for efficient cell death: characterization of cells infected with adp mutants. Virology 220, 152–162.
Tollefson, A.E., Scaria, A., Hermiston, T.W., Ryerse, J.S., Wold, L.J., Wold, W.S., 1996b. The adenovirus death protein (E3-11.6K) is required at very late stages of infection for efficient cell lysis and release of adenovirus from infected cells. J. Virol. 70, 2296–2306.
Tollefson, A.E., Toth, K., Doronin, K., Kuppuswamy, M., Doronina, O.A., Lichtenstein, D.L., Hermiston, T.W., Smith, C.A., Wold, W.S., 2001. Inhibition of TRAIL-induced apoptosis and forced internalization of TRAIL receptor 1 by adenovirus proteins. J. Virol. 75, 8875–8887.
Walsh, M.P., Seto, J., Jones, M.S., Chodosh, J., Xu, W., Seto, D., 2010. Computational analysis identifies human adenovirus type 55 as a re-emergent acute respiratory disease pathogen. J. Clin. Microbiol. 48, 991–993.
Windheim, M., Honing, S., Leppard, K.N., Butler, L., Seed, C., Ponnambalam, S., Burgert, H.G., 2016. Sorting motifs in the cytoplasmic tail of the immunomodulatory E3/49K protein of species D adenoviruses modulate cell surface expression and ectodomain shedding. J. Biol. Chem. 291, 6796–6812.
Windheim, M., Southcombe, J.H., Kremmer, E., Chaplin, L., Urlaub, D., Falk, C.S., Claus, M., Mihm, J., Braithwaite, M., Dennehy, K., Renz, H., Sester, M., Watzl, C., Burgert, H.G., 2013. A unique secreted adenovirus E3 protein binds to the leukocyte common antigen CD45 and modulates leukocyte functions. Proc. Natl. Acad. Sci. U.S.A. 110, E4884–E4893.
Wo, Y., Lu, Q.B., Huang, D.D., Li, X.K., Guo, C.T., Wang, H.Y., Zhang, X.A., Liu, W., Cao, W.C., 2015. Epidemical features of HAdV-3 and HAdV-7 in pediatric pneumonia in Chongqing, China. Arch. Virol. 160, 633–638.
Yamamoto, D., Okamoto, M., Lupisan, S., Suzuki, A., Saito, M., Tamaki, R., Tandoc 3rd, A., Mercado, E., Sombrero, L., Olveda, R., Oshitani, H., 2014. Impact of human adenovirus serotype 7 in hospitalized children with severe fatal pneumonia in the Philippines. Jpn. J. Infect. Dis. 67, 105–110.
Zhang, Q., Jing, S., Cheng, Z., Yu, Z., Dehghan, S., Shamsaddini, A., Yan, Y., Li, M., Seto, D., 2017. Comparative genomic analysis of two emergent human adenovirus type 14 respiratory pathogen isolates in China reveals similar yet divergent genomes. Emerg. Microb. Infect. 6, e92.
Zou, A., Atencio, I., Huang, W.M., Horn, M., Ramachandra, M., 2004. Overexpression of adenovirus E3-11.6K protein induces cell killing by both caspase-dependent and caspase-independent mechanisms. Virology 326, 240–249.